# An ultrafiltration- reverse osmosis combined process for external reuse of Weiyuan shale gas flowback and produced water

Can Guo,[a,b,1] Haiqing Chang,[a,b,1] Baicang Liu,[a,b,*] Qiping He,[c] Boya Xiong,[d] Manish Kumar[d] and Andrew L. Zydney[e]

[a] Key Laboratory of Deep Underground Science and Engineering (Ministry of Education), Institute of New Energy and Low-Carbon Technology, Sichuan University, Chengdu 610207, China

[b] College of Architecture and Environment, Sichuan University, Chengdu, Sichuan 610207, PR China

[c] Chuanqing Drilling Engineering Company Limited, Chinese National Petroleum Corporation, Chengdu 610081, PR China

[d] Department of Civil and Environmental Engineering, The Pennsylvania State University, Greenberg Building, University Park, PA, 16802, United States

[e] Department of Chemical Engineering, The Pennsylvania State University, Greenberg Building, University Park, PA, 16802, United States

## Supporting Information:

10 pages

9 figures

1 table

* Corresponding author. Tel.: ＋86 28 85995998; fax: +86 28 62138325.
E-mail address: bcliu@scu.edu.cn (B. Liu).

[1]These authors contributed equally to this work.

## S1. Scaling potential in the RO unit

The Stiff and Davis saturation index (S&DSI) was used to evaluate the scaling potentials in RO units. S&DSI is defined as the difference between the measured pH and the saturation $pH_S$:[1-3]

$$\text{S\&DSI} = \text{pH} - \text{pH}_S \tag{S1}$$

$$\text{pH}_S = \text{pCa}^{2+} + \text{pAlK} + K \tag{S2}$$

where pH is the actual solution pH and $pH_S$ is the pH at saturation; $pCa^{2+}$ and pAlk are the negative of the logarithm of the calcium ion concentration and of the alkalinity, respectively, and $K$ is a factor that accounts for the ionic strength and temperature of the solution.

For the RO influent (i.e, UF permeate), the variations of S&DSI with the RO recovery is shown in **Fig. S1**. The positive values of S&DSI indicate the likely formation of scaling during RO treatment.

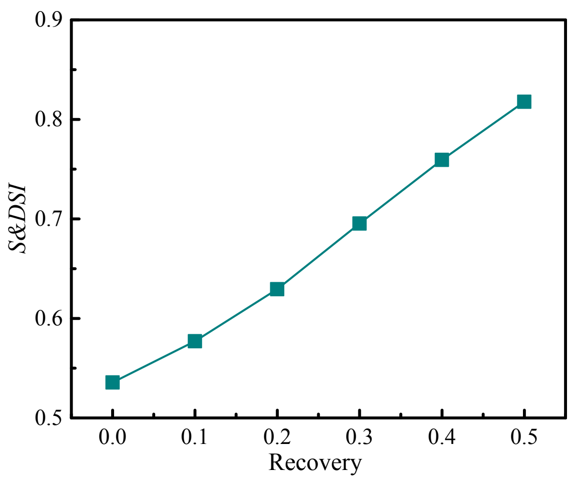


**Fig. S1** Scaling potentials (S&DSI) as a function of the RO recovery.

**S2. Variations of turbidity and COD in UF permeate**

**Fig. S2** presents the changes in turbidity and COD of the UF permeate during filtration at a flux of 50 L/(m$^2$·h). The turbidity and COD were both essentially constant throughout the UF, with only slight variations with the filtrate volume (i.e., filtration time).

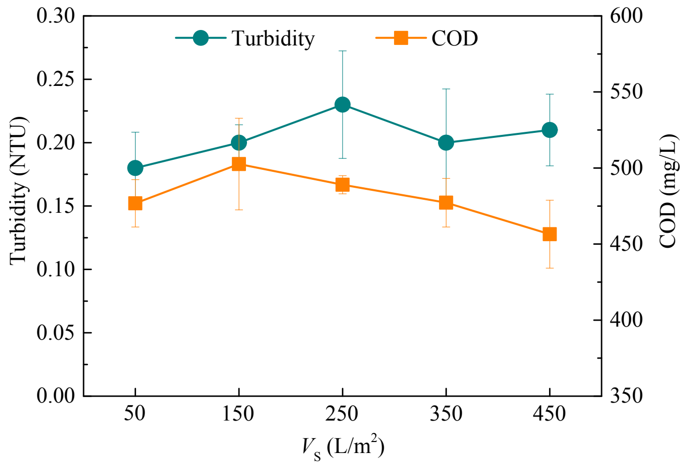


**Fig. S2.** Variations of turbidity and COD in UF permeate (Flux: 50 L/(m$^2$·h)).

**S3. Characteristics of the FPW and its effluent after different treatments**

**Table S1**

Characteristics of the UF feed and its effluent after different treatments.

| Constituents | UF feed | UF permeate[b] | RO permeate[c] | | | |
|---|---|---|---|---|---|---|
| | | | 2.5 MPa | 3.5 MPa | 4.5 MPa | 5.5 MPa |
| Turbidity (NTU) | 49.8 | 0.19 | 0.09 | 0.06 | 0.07 | 0.05 |
| TSS (mg/L) | 55.4 | - | - | - | - | - |
| TDS (mg/L) | 18,900 | 18,500 | 1040 | 361 | 192 | 172 |
| Conductivity (mS/cm) | 31.14 | 30.75 | 2.29 | 0.76 | 0.41 | 0.37 |
| Alkalinity (as $CaCO_3$, mg/L) | 600 | 490 | - | - | - | - |
| COD (mg/L) | 530 | 481 | 16.4 | 10.9 | 7.5 | 6.0 |
| pH | 7.16 | 8.39 | 8.12 | 7.98 | 8.04 | 7.91 |
| Total Fe (mg/L) | 2.49 | 2.45 | 0.62 | 0.46 | 0.28 | 0.15 |
| Total Cu (mg/L) | 6.50 | 5.88 | 0.43 | 0.38 | 0.22 | 0.09 |
| $Na^+$ (mg/L) | 6,950 | 6870 | 258 | 141 | 76.1 | 66.8 |
| $Ca^{2+}$ (mg/L) | 233 | 229 | 3.02 | 1.27 | 0.59 | 0.36 |
| $Mg^{2+}$ (mg/L) | 26.9 | 25.7 | 0.40 | 0.11 | 0.05 | 0.04 |
| $K^+$ (mg/L) | 134.5 | 129.7 | 6.50 | 2.74 | 1.31 | 1.27 |
| $Sr^{2+}$ (mg/L) | 72.9 | 64.2 | 0.75 | 0.22 | 0.09 | 0.06 |
| $Ba^{2+}$ (mg/L) | 135 | 133 | 2.23 | BDL | BDL | BDL |
| $NH_4^+$ (mg/L) | 92.0 | 89.9 | 6.59 | 3.99 | 2.37 | 2.27 |
| $Mn^{2+}$ (mg/L) | BDL[a] | BDL | BDL | BDL | BDL | BDL |
| $Cl^-$ (mg/L) | 11,000 | 10900 | 627 | 190 | 97 | 87 |
| $SO_4^{2-}$ (mg/L) | 12.1 | 11.9 | 0.31 | 0.10 | 0.08 | 0.06 |
| $F^-$ (mg/L) | 2.41 | 1.94 | 0.09 | 0.03 | 0.02 | 0.02 |
| $Br^-$ (mg/L) | 61.0 | 60.4 | 3.65 | 1.23 | 0.65 | 0.59 |
| $NO_2^-$ (mg/L) | 7.74 | 6.98 | 0.69 | 0.15 | 0.12 | 0.10 |

[a]Below the detection limit (0.01 mg/L).

[b]The UF membrane permeate was obtained under the flux of 50 L/($m^2 \cdot h$).

[c]The water recovery was 30%.

## S4. Role of backwash conditions on UF membrane fouling and verification of critical flux

UF tests with different backwash parameters were carried out. The experimental protocol was the same as that used for the UF tests described in the manuscript, except for the backwash parameters. A filtration flux of 50 LMH was employed for all tests, and the same volume of backwash water was used. **Fig. S3** shows the comparison of TFI of UF membranes under different backwash conditions. As presented in **Figs. S3a-b**, there was no statistically significant difference in the calculated values of TFI ($p > 0.05$) when the backwash volume was constant. Previous literature on UF of seawater also indicated that backwashing with permeate water resulted in a similar final TMP when the backwash interval (i.e., filtration duration) was not too large.[4]

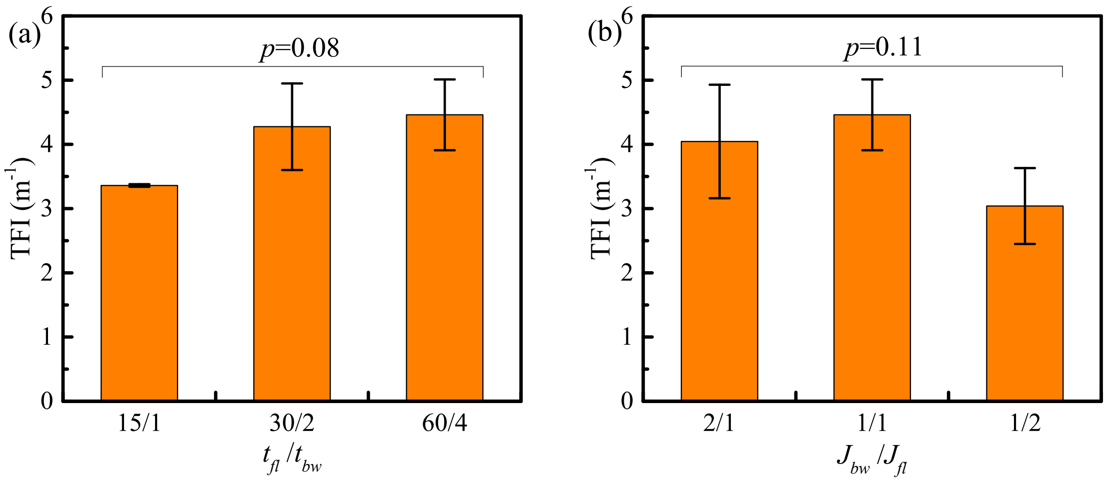


**Fig. S3.** Comparison of TFI under different backwash conditions with the same volume of backwash water: (a) effect of backwash duration (by maintaining a constant ratio of $t_{fl}$ and $t_{bw}$, $t_{fl}/t_{bw}$=15, $J_{fl} = J_{bw}$ = 50 LMH), and (b) effect of backwash flux ($t_{fl}$ = 60 min, $J_{fl}$ = 50 LMH; $J_{bw}/J_{fl}$ = 2/1, 1/1, 1/2, and corresponding $t_{bw}$ = 2, 4, 8 min) (Note: $t_{fl}$ = filtration duration, $t_{bw}$ = backwash duration, $J_{fl}$ = filtration flux = 50

LMH, $J_{bw}$ = backwash flux).

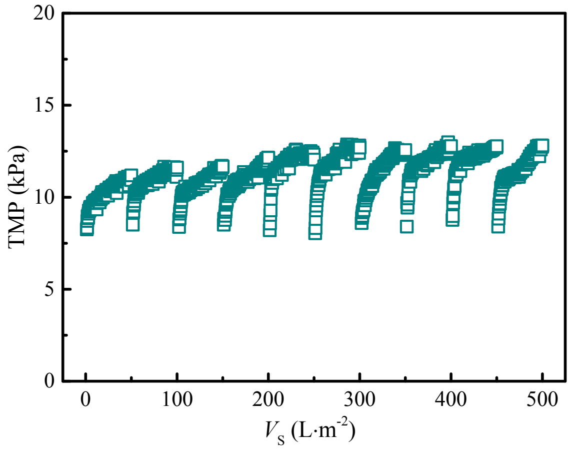


**Fig. S4.** UF membrane fouling at a flux of 15 LMH.

## S5. RO flux and its decline with recovery

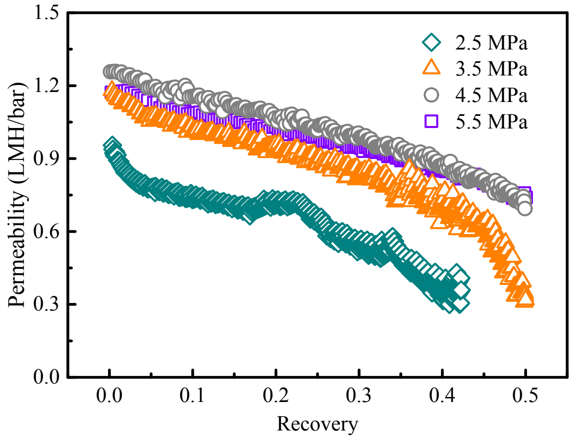


**Fig. S5.** Plot of RO permeate flux per net pressure driving force as function of recovery.

The flux decline ($\Delta J$) in the RO unit was calculated by subtracting the measured flux from the pure water flux. Using Eq. (7) in the manuscript, the flux values can be determined by product of hydraulic permeability and osmotic pressure differential, and subtracting these fluxes from the pure water flux led to the flux decline due to osmotic pressure ($\Delta J_{osmotic\ pressure}$). Thus, the ratio of flux decline due to osmotic pressure to RO flux decline was determined, as presented in **Fig. S6**.

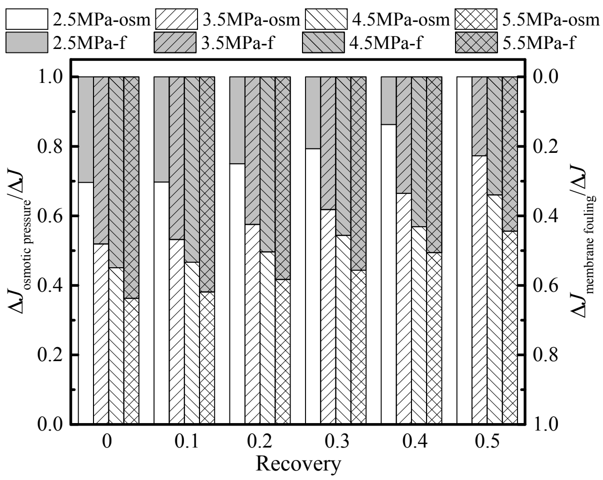


**Fig. S6.** The ratio of flux decrease due to osmotic pressure in total RO decline flux under different recoveries and pressures (In legend, osm: osmotic pressure; f: membrane fouling).

## S6. Determination of solute permeability coefficient

**Figs. S7-S8** present the plot of permeate flux as a function of rejection for RO system to determine the solute permeability for TDS and COD of Weiyuan shale gas FPW, respectively. The solute permeability coefficients $\omega$ determined using linear regression were $5.1\times10^{-8}$ and $8.4\times10^{-8}$ m/s for TDS and COD, respectively.

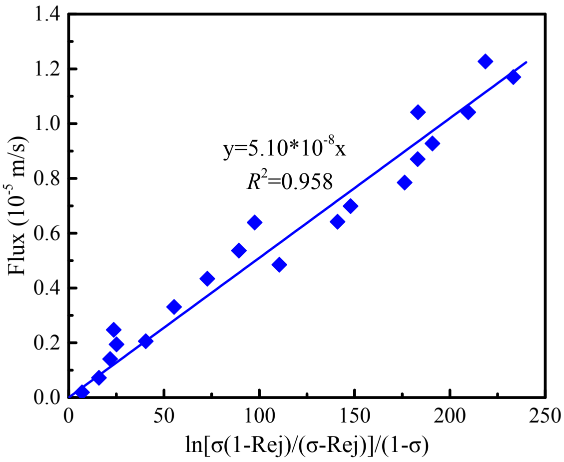


**Fig. S7.** Plot of permeate flux as a function of TDS rejection for RO system to determine the solute permeability of Weiyuan shale gas FPW.

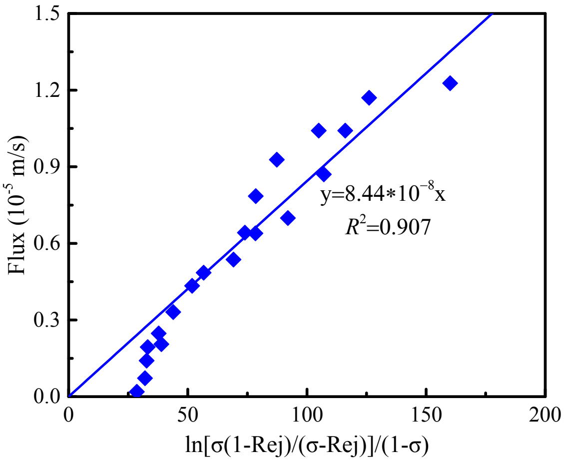


**Fig. S8.** Plot of permeate flux as a function of COD rejection for RO system to determine the solute permeability of Weiyuan shale gas FPW.

## S7. Specific energy consumption of RO unit

The specific energy consumption (*SEC*) and normalized SEC ($SEC_{norm}$) for a single-pass RO process were calculated using Eqs. (S4)-(S5):[5]

$$SEC = \triangle P/r \tag{S4}$$

$$SEC_{norm} = R_{ej}/r(1-r) \tag{S5}$$

The SEC and normalized SEC under different recoveries and pressures are illustrated in **Fig. S9**. As presented in **Fig. S9a**, when the recoveries of RO step were 0.3-0.5, the SEC values ranged from 1.4 to 5.1 kWh/m$^3$. These values are consistent with literature reports showing that the SEC was 2.5-7.0 kWh/m$^3$ for RO treatment of shale gas FPW.[6-10]

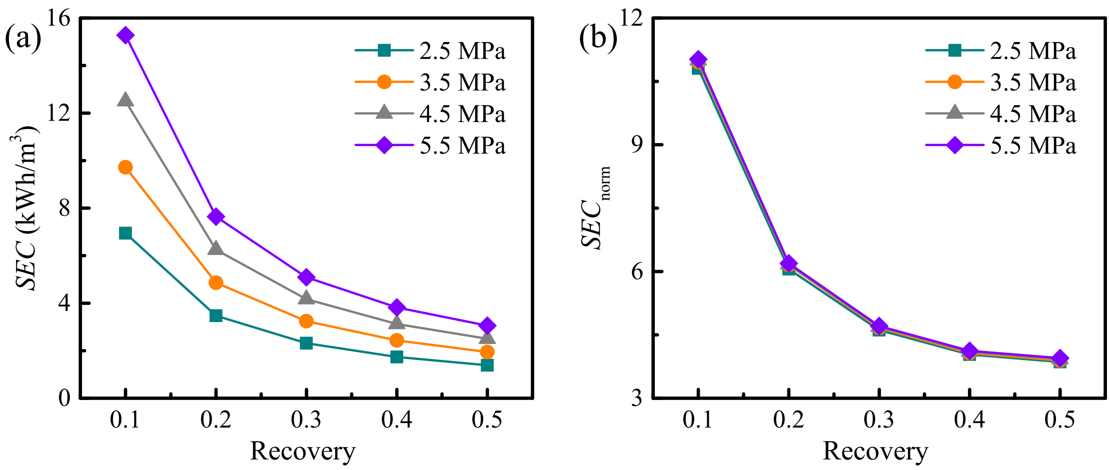


**Fig. S9.** The SEC and normalized SEC of RO unit under different recoveries and pressures

## References

1. A. Antony, J. H. Low, S. Gray, A. E. Childress, P. Le-Clech and G. Leslie, Scale formation and control in high pressure membrane water treatment systems: A review, *J. Membr. Sci.*, 2011, **383**, 1-16.

2. L. N. Sim, T. H. Chong, A. H. Taheri, S. T. V. Sim, L. Lai, W. B. Krantz and A. G. Fane, A review of fouling indices and monitoring techniques for reverse osmosis, *Desalination*, 2018, **434**, 169-188.
3. J. Peña, B. Buil, A. Garralón, P. Gómez, M. J. Turrero, A. Escribano, G. Garralón and M. A. Gómez, The vaterite saturation index can be used as a proxy of the S&DSI in sea water desalination by reverse osmosis process, *Desalination*, 2010, **254**, 75-79.
4. A. Resosudarmo, Y. Ye, P. Le-Clech and V. Chen, Analysis of UF membrane fouling mechanisms caused by organic interactions in seawater, *Water Res.*, 2013, **47**, 911-921.
5. A. Zhu, P. D. Christofides and Y. Cohen, Minimization of energy consumption for a two-pass membrane desalination: Effect of energy recovery, membrane rejection and retentate recycling, *J. Membr. Sci.*, 2009, **339**, 126-137.
6. J. Kim, J. Kim, J. Kim and S. Hong, Osmotically enhanced dewatering – reverse osmosis (OED – RO) hybrid system: Implications for shale gas produced water treatment, *J. Membr. Sci.*, 2018, **554**, 282–290.
7. G. P. Thiel, E. W. Tow, L. D. Banchik, H. W. Chung and J. H. Lienhard, Energy consumption in desalinating produced water from shale oil and gas extraction, *Desalination*, 2015, **366**, 94-112.
8. B. D. Coday, L. Miller-Robbie, E. G. Beaudry, J. Munakata-Marr and T. Y. Cath, Life cycle and economic assessments of engineered osmosis and osmotic dilution for desalination of Haynesville shale pit water, *Desalination*, 2015, **369**, 188-200.
9. H. R. Acharya, C. Henderson, H. Matis, H. Kommepalli, B. Moore and H. Wang, *Cost effective recovery of low-TDS Frac Flowback water for re-use: Final Report*, U.S. Department of Energy, Washington, DC, 2011.
10. R. Hammer, J. VanBriesen and L. Levine, *In fracking's wake new rules are needed to protect our health and environment from contaminated wastewater*, 2012.